

Two different carbon-hydrogen complexes in silicon with closely spaced energy levels

R. Stübner,^{a)} V. Kolkovsky,^{a)} and J. Weber

Technische Universität Dresden, Institut für Angewandte Physik, 01062 Dresden, Germany

(Received 12 June 2015; accepted 24 July 2015; published online 7 August 2015)

An acceptor and a single donor state of carbon-hydrogen defects (CH_A and CH_B) are observed by Laplace deep level transient spectroscopy at 90 K. CH_A appears directly after hydrogenation by wet chemical etching or hydrogen plasma treatment, whereas CH_B can be observed only after a successive annealing under reverse bias at about 320 K. The activation enthalpies of these states are 0.16 eV for CH_A and 0.14 eV for CH_B . Our results reconcile previous controversial experimental results. We attribute CH_A to the configuration where substitutional carbon binds a hydrogen atom on a bond centered position between carbon and the neighboring silicon and CH_B to another carbon-hydrogen defect. © 2015 AIP Publishing LLC.

[<http://dx.doi.org/10.1063/1.4928146>]

INTRODUCTION

Hydrogen is an inadvertent contamination during many processing and growth processes of semiconductors. Hydrogen passivates electrical active defects but also creates new electronic levels. In crystalline silicon an activation of isoelectronic, neutral substitutional carbon was detected in 1989.¹ The nature of this defect, which is important for devices in Czochralski or float-zone materials, was discussed controversially later on.

The CH complex was first expected to reflect the principal electronic properties of isolated H.^{1,2} In contrast, the results of Ref. 3 showed that the presence of carbon near H altered significantly the electrical properties of H in the CH complex. The CH complex forms a positive- U sequence of levels, where the single acceptor level lies closer to the conduction band compared to the single donor level. Theory calculates a bond-centered position for H between substitutional C and a neighboring Si crystal site (CH_{IBC}) as the most stable configuration for the positive and neutral charge states.^{3–5} However, for the negative charge state, the results are ambiguous. According to the results of Ref. 3, CH_{IBC} should be also stable in its negative charge state, whereas the tetrahedral interstitial configuration of H (CH_{Td}) and the antibonding interstitial position of H at the carbon atom (CH_{IAB}) were found to be stable in Refs. 4 and 5. The acceptor state of CH_{IBC} should be located around $E_C - 0.3$ eV, whereas its donor state was calculated at around $E_V + 0.31$ eV.^{3,6} The level positions of the CH_{Td} and CH_{IAB} were also calculated as $E_C - 0.89$ eV and $E_C - 0.63$ eV, respectively.³

Experimental evidence for the single acceptor and single donor level of the bond centered CH complex is controversial. Previously, a dominant deep level transient spectroscopy (DLTS) peak at about 90 K was observed in n -type Si and assigned to the single donor state of CH_{IBC} .^{1,7,8} In those studies, the samples (CZ and FZ) were hydrogenated either

by wet chemical etching or by a hydrogen plasma treatment at 150 °C. However, before the DLTS measurements always an annealing at 320 K for a couple of hours under a reverse bias of -4 V (reverse bias annealing, RBA) was performed.^{1,7,8} The single donor level was observed only after the RBA treatment, which was concluded to be necessary in order to increase the initial hydrogen concentration in the depletion layer. The activation enthalpy of this defect was obtained as $E_C - 0.16$ eV, whereas the capture cross section was about $\sigma = 7 \times 10^{-16} \text{ cm}^2$. The authors observed the typical enhancement of the emission rate with electric field.⁹ These arguments together with the positive additional charge observed in the capacitance-voltage (C - V) profile allowed the authors to assign the CH level to a single donor state of CH. A defect level with similar energies was also reported by Yoneta *et al.*¹⁰ However, in contrast to Endrös *et al.*, an enhancement of the emission rate for the level was not detected. We also notice that the measurements in Ref. 10 were performed directly after hydrogenation of their samples and no RBA treatment was used. The thermal stability of the level studied by Kamiura *et al.*⁶ gave different dissociation energies of this defect inside (0.7 eV) and outside (1.3 eV) the depletion region. It was concluded that the CH complex became unstable in the neutral charge state by capturing an electron, which was less likely inside the depletion region.

Andersen *et al.* reported on a combined experimental and theoretical study on the electrical and structural properties of the CH complex.³ Using the high-resolution Laplace DLTS¹¹ technique, a single level labeled $(\text{CH})_{\text{II}}$ was observed directly after H implantation or wet chemical etching at about 90 K in FZ Si. The activation enthalpy and capture cross section of this defect were similar to those presented for the CH complex in Refs. 1 and 10. However, based on the absence of the Poole-Frenkel effect, $(\text{CH})_{\text{II}}$ was assigned to an acceptor state. From Laplace DLTS measurements under uniaxial stress, a trigonal symmetry of $(\text{CH})_{\text{II}}$ was obtained. This defect was found to be stable slightly above room temperature. In addition to $(\text{CH})_{\text{II}}$, another level of the CH complex, labeled $(\text{CH})_{\text{I}}$, was also reported in

^{a)}Authors to whom correspondence should be addressed. Electronic addresses: ronald.stuebner@physik.tu-dresden.de and kolkov@ifpan.edu.pl

Ref. 3. The activation enthalpy of $(\text{CH})_{\text{I}}$ was found to be 0.22 eV, and a capture cross section was $2 \times 10^{-14} \text{ cm}^2$. This level was shown to be a single donor, and it was stable up to 225 K in *n*-type Si. During its annealing, a direct conversion between $(\text{CH})_{\text{I}}$ and $(\text{CH})_{\text{II}}$ was reported in Ref. 3. This conversion was interpreted with an atomic reconfiguration of H from a bond-centered position at the second-nearest neighbor of a substitutional carbon atom ($\text{CH}_{2\text{BC}}$) to a bond-centered position next to the carbon atom ($\text{CH}_{1\text{BC}}$).

In the present study, we shed light on the controversy of the charge states and structures of the dominant CH-related defects. We will show that two different defects exist in *n*-type Si depending on the treatment of hydrogenated samples. The origin of these defects will be discussed.

EXPERIMENTAL PROCEDURE

The samples investigated were [100] and [111] oriented *FZ* crystals doped with phosphorous in the range of $1 \times 10^{14} \text{ cm}^{-3}$ to $9 \times 10^{15} \text{ cm}^{-3}$. Carbon was unintentionally introduced during growth, and its concentration was around $5 \times 10^{15} \text{ cm}^{-3}$ as obtained from infrared spectroscopy measurements. Hydrogen was introduced by wet chemical etching at room temperature for 3 min in an acid consisting of $\text{HNO}_3\text{:HF:CH}_3\text{COOH}$ with the volume ratio of 5:3:3. For some samples, hydrogenation was performed by exposure to a dc H-plasma at 40 °C for 30 min. Schottky diodes were produced by evaporation of Au in vacuum onto the polished side of the samples at room temperature. Ohmic contacts were prepared by rubbing the back side of the samples with a eutectic InGa alloy. The Schottky and Ohmic contacts were characterized by current-voltage (*I-V*) and capacitance-voltage (*C-V*) measurements in the range of 80–300 K. Some samples were subjected to RBA with a reverse bias of -2 V to -4 V for several hours at 320 K. After RBA, the samples were cooled under reverse bias below 90 K before the measurements started. Some samples received an anneal at 320 K with short-circuited contacts (zero bias annealing, ZBA). After ZBA, the samples were cooled below 90 K without a reverse bias. *C-V* measurements were performed at 1 MHz with a Boonton 7200 capacitance meter. Double Laplace DLTS¹¹ with two filling pulses was employed to investigate the deep levels. Deep level profiles were measured at a fixed reverse bias while varying the biases of the two filling pulses. The electrical field was calculated from the *C-V* profiles as described in Ref. 12. The influence of the electric field on the emission rate was determined by varying the reverse bias while keeping the bias of the two filling pulses fixed.

EXPERIMENTAL RESULTS AND DISCUSSION

Figure 1 shows Laplace DLTS spectra recorded at 85 K in samples with different net donor concentrations after reverse bias annealing at 320 K for 8 h as in Refs. 1, 7, and 8. The reverse bias during the measurements was chosen such that the electric field strength in the investigated region was identical. The biases of the filling pulses were varied in such a way that the investigated region covered the edge of the depletion region during the RBA treatment. In samples

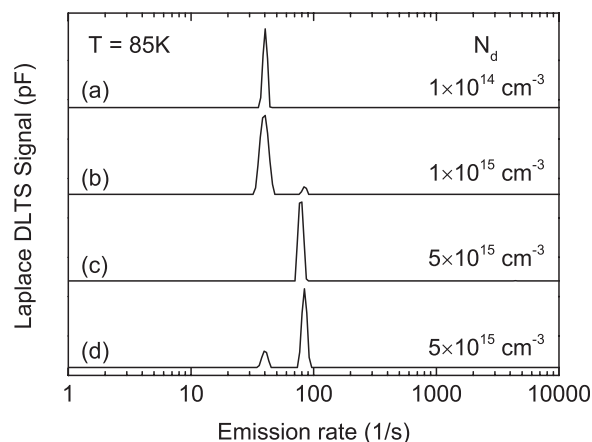


FIG. 1. Laplace DLTS spectra recorded at 85 K after RBA in samples with different net free-carrier concentrations.

with a net free carrier concentration of $1 \times 10^{14} \text{ cm}^{-3}$, a single Laplace DLTS peak, labeled CH_A , was observed after RBA (a). In samples with a net donor concentration of $1 \times 10^{15} \text{ cm}^{-3}$ besides CH_A another small Laplace DLTS peak, labeled CH_B , with an emission rate shifted towards higher values as compared to CH_A , was observed after RBA treatment (b). We also notice that only CH_A was observed in these samples directly after hydrogenation. After RBA only CH_B could be observed close to the edge of the depletion region in samples with a net donor concentration of $5 \times 10^{15} \text{ cm}^{-3}$ (c). However, if the probed region is shifted towards the surface CH_A could be also detected (d).

The same defects CH_A and CH_B were observed in [100] and [111] oriented wafers. This indicates that an anisotropy of the defect potential cannot be the origin of the shift between the emission rates of CH_A and CH_B .

Figure 2 presents Laplace DLTS spectra of CH_A and CH_B recorded at different values of the reverse bias. By changing the reverse bias applied to the diode from -2 V to -10 V , the emission rate for CH_A is only slightly changed (Fig. 2(a)). In contrast, the changes for CH_B are more pronounced (Fig. 2(b)). Figure 3(a) shows the plot of the emission rate of CH_A and CH_B as a function of the square root of the electric field. This plot summarizes our results obtained from different samples with different net doping concentrations. As mentioned above, the changes of the emission rate of CH_B with electric field are significantly stronger compared to those observed for CH_A .

In order to analyze these changes, quantitatively different models were used. A defect with an attractive Coulomb potential should exhibit an increase in the emission rate e with the applied electric field E by the barrier lowering according to the Poole-Frenkel model^{9,13}

$$e = e_0 \exp(\beta \sqrt{E} / 2kT), \quad (1)$$

with e_0 being the emission rate without field and $\beta = (q^3 / \pi \epsilon_r \epsilon_0)^{1/2}$, q is the electronic charge, and ϵ_r and ϵ_0 are the relative and the vacuum permittivity, respectively. The enhancement of the emission rate of electrons or holes bound to neutral defects can be satisfactorily described by a

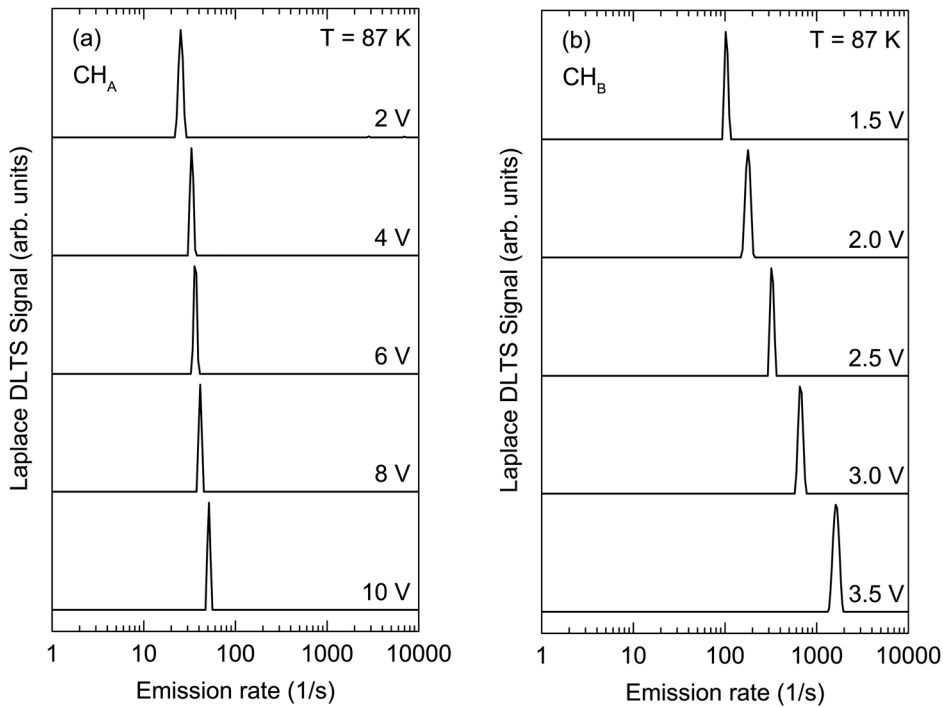


FIG. 2. Laplace DLTS spectra recorded with different reverse biases in as-grown Si immediately after hydrogenation (a) and after a following RBA treatment at 320 K with -2 V (b).

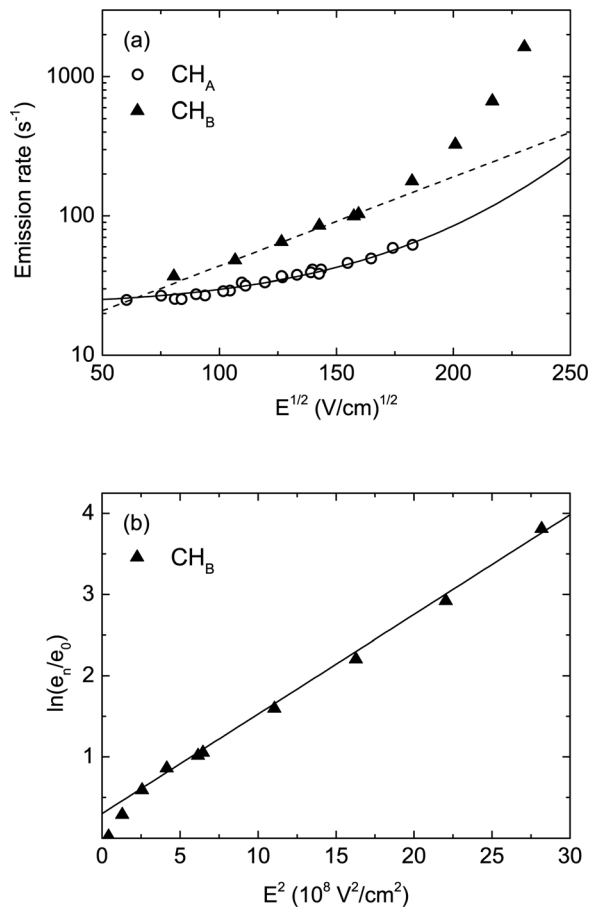


FIG. 3. (a) The emission rate of defects observed before (CH_A) and after (CH_B) the RBA treatment as a function of the square root of the electric field. The results of the calculation within the Poole-Frenkel model for a defect with a Coulombic potential are shown as a dashed line. The fit of the experimental data of CH_A with a square-well potential is shown as solid line. Emission rates of CH_B versus the square of the electric field are presented in (b). The solid line shows a linear fit of the experimental data for electric fields above 2×10^4 V/cm.

square-well potential. In this case, the field dependence of the emission rate varies according to⁹

$$e = e_0 \left[(2\gamma E)^{-1} (\exp(\gamma E) - 1) + \frac{1}{2} \right], \quad (2)$$

where $\gamma = qr/kT$ and r is the radius of the square-well potential.

The dashed line in Fig. 3(a) shows the fit to the Poole-Frenkel model for the experimental emission rates of CH_B . Excellent agreement is obtained for electric fields below 170 (V/cm) $^{1/2}$. For higher electric fields, the emission rate increases stronger than that predicted by the Poole-Frenkel model. This is a well-known phenomenon which is commonly explained by the contribution of phonon-assisted tunneling to the carrier emission.¹⁴ If the phonon-assisted tunneling becomes dominant, the logarithm of the emission rate of a defect should follow the square of the electric field. This was indeed observed for CH_B (Fig. 3(b)). In contrast, the enhancement of the emission rate of CH_A is much weaker than that predicted for a defect with a Coulombic potential. However, the experimental data can be well described by a square-well potential with a radius of $r = 5.5$ nm (solid line in Fig. 3(a)).

The activation enthalpies of CH_A and CH_B as determined from the Arrhenius plots were found as 0.16 eV and 0.14 eV, respectively. These values are identical to those previously reported for CH complexes observed after implantation and after a RBA treatment at 320 K in Refs. 1, 3, 7, and 8, respectively.

In order to shed light on the origin of the observed defects, their depth profiles are analyzed. The depth profile of CH_A recorded after hydrogenation by wet chemical etching is shown in Fig. 4. This profile was also compared with that of the phosphorus-hydrogen (PH) complex which was

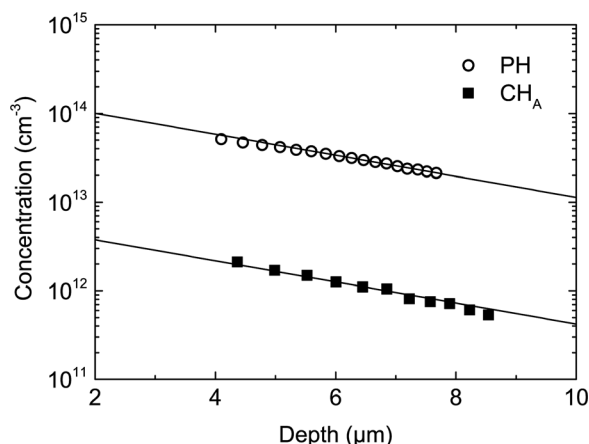


FIG. 4. Comparison of the depth profiles of CH_A and PH recorded directly after hydrogenation by wet chemical etching in samples with a net free-carrier concentration of $1 \times 10^{14} \text{ cm}^{-3}$.

obtained by subtraction of the phosphorus donor concentration after hydrogenation from the net free carrier concentration in as-grown samples. Two characteristic features of the profiles can be distinguished. The concentration of PH is a factor of 20–50 higher as compared to CH_A . However, the reduction of the concentration of these defects towards the bulk of the sample was found to be identical. According to Ref. 15, our results indicate that both complexes contain the same number of hydrogen atoms.

Depth profiles of the CH_A and CH_B defects in samples with different free carrier concentrations after a subsequent RBA treatment are shown in Fig. 5. As mentioned above in samples with a net donor concentration of $1 \times 10^{15} \text{ cm}^{-3}$, CH_A is observed and its concentration decreases similarly as the PH concentration (Fig. 5(a)). In contrast, the decrease of CH_B with depth is significantly stronger compared to that of PH in samples with a net donor concentration of $1 \times 10^{16} \text{ cm}^{-3}$ (Fig. 5(b)). The different slopes of the CH_A and CH_B profiles could suggest that CH_A and CH_B contain different numbers of H atoms.

Our results confirm that two different CH-related defects are created in the depletion region depending on the processing treatment of C-doped Si. CH_A appears directly in samples after their hydrogenation by wet chemical etching or by a dc H-plasma. The electrical parameters of this defect are

identical to those of $(\text{CH})_{\text{II}}$ reported by Andersen *et al.*³ The reported absence of a field effect for $(\text{CH})_{\text{II}}$ can be explained by the small electric field in comparison to that employed in the present study. Indeed, the changes of the emission rate of CH_A were found to be less than 10% if the electric field varies below $100 (\text{V/cm})^{1/2}$. The good agreement of our experimental data with a square-well potential of a radius $r = 5.5 \text{ nm}$ (Fig. 3) is consistent with the single acceptor nature of this defect. Similar values for the radius were previously reported for other point defects with potentials which describe an interaction without an attractive force and therefore are either neutral or equally charged as the emitted carrier after the emission.^{16,17}

In contrast, CH_B can be detected only in C-doped Si samples subjected to an additional RBA treatment at around 300–350 K after their hydrogenation. The electrical properties, including the enhancement of the emission rate of this configuration, are identical to those reported in Refs. 1 and 7. Therefore, we identify CH_B with the CH level observed by Endrös in Ref. 1. An adequate fit of the enhancement of the emission rate of CH_B can be obtained using the Poole-Frenkel model which is valid for defects with an attractive Coulombic potential. In good agreement with Refs. 1 and 7, we identify CH_B with the single donor state of a CH-related defect.

Now we address the question as to the origin of CH_A and CH_B . In Ref. 3, the single acceptor state of $(\text{CH})_{\text{II}}$ or in our labeling CH_A was assigned to the CH_{IBC} configuration, where hydrogen sits at a bond-centered position between carbon and a neighboring silicon atom. As mentioned above, this assignment was based on the comparison of the calculated electronic properties of CH_{IBC} with those of $(\text{CH})_{\text{II}}$ from Ref. 1. Uniaxial stress measurements also confirmed the trigonal symmetry of this defect.^{3,18} In addition, the findings of the present study show that CH_A indeed contains only one H atom. Therefore, it seems reasonable to ascribe this defect to CH_{IBC} .

As shown above, CH_B is identical to the defects observed in Refs. 1, 7, and 8. It usually appears in hydrogenated *n*-type Si after an additional RBA treatment. The concentration of this defect depends on C and H concentrations, and therefore, it is likely a CH defect. However, the depth profiles for this defect showed a stronger decrease as

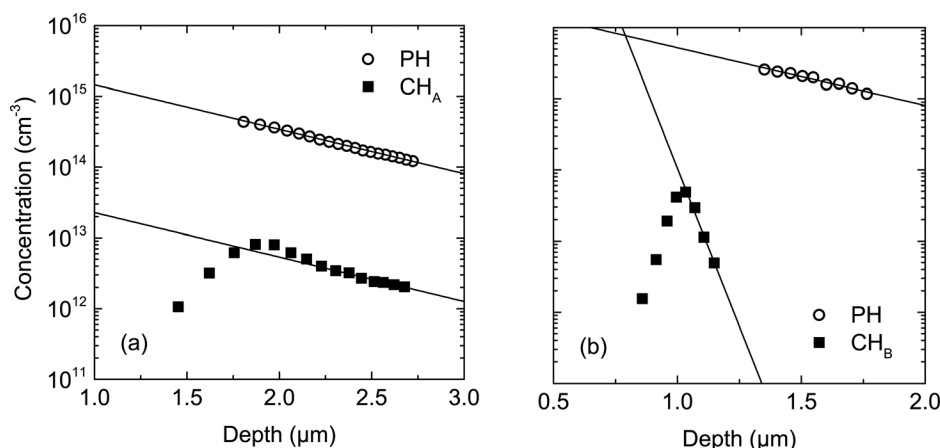


FIG. 5. Comparison of the depth profiles of CH_A and CH_B with those of PH recorded after a RBA treatment in samples with net free-carrier concentrations of $1 \times 10^{15} \text{ cm}^{-3}$ (a) and $1 \times 10^{16} \text{ cm}^{-3}$ (b).

compared to PH and CH_A. In addition, we do not observe any reorientation between CH_A and CH_B by annealing the samples between 280 and 350 K without applied reverse bias. Therefore, we tentatively attribute CH_B to a CH defect which contains more than one H atom. Unfortunately, from our studies, we were not able to determine the number of H atoms in CH_B. Theoretical calculations should help to understand the structure of the CH_B defect.

CONCLUSIONS

In the present study, we determined that two different CH defects (CH_A and CH_B) can be observed at 90 K in *n*-type Si. From the analysis of their emission-rate dependence on the electric field, we assign CH_A to a single acceptor and CH_B to a single donor state. From the depth profiles of the defects, we attribute CH_A to the single acceptor state of CH_{1BC} with a H atom located in the bond-centered position close to a C atom whereas CH_B was tentatively correlated with a CH-related defect containing a higher number of H atoms compared to CH_A.

¹A. Endrös, *Phys. Rev. Lett.* **63**, 70–73 (1989).

²S. T. Pantelides, *Appl. Phys. Lett.* **50**, 995–997 (1987).

- ³O. Andersen, A. R. Peaker, L. Dobaczewski, K. B. Nielsen, B. Hourahine, R. Jones, P. R. Briddon, and S. Öberg, *Phys. Rev. B* **66**, 235205 (2002).
- ⁴C. Kaneta and H. Katayama-Yoshida, *Mater. Sci. Forum* **196–201**, 897–902 (1995).
- ⁵P. Leary, R. Jones, and S. Öberg, *Phys. Rev. B* **57**, 3887–3899 (1998).
- ⁶Y. Kamiura, M. Tsutsue, Y. Tamashita, F. Hashimoto, and K. Okuno, *J. Appl. Phys.* **78**, 4478 (1995).
- ⁷A. L. Endrös, W. Krühler, and F. Koch, *J. Appl. Phys.* **72**, 2264–2271 (1992).
- ⁸W. Cszaszar and A. L. Endrös, *Phys. Rev. Lett.* **73**, 312–315 (1994).
- ⁹J. L. Hartke, *J. Appl. Phys.* **39**, 4871 (1968).
- ¹⁰M. Yoneta, Y. Kamiura, and F. Hashimoto, *J. Appl. Phys.* **70**, 1295–1308 (1991).
- ¹¹L. Dobaczewski, A. R. Peaker, and K. B. Nielsen, *J. Appl. Phys.* **96**, 4689–4728 (2004).
- ¹²P. Blood and P. W. Orton, *The Electrical Characterization of Semiconductors: Majority Carriers and Electron States* (Academic Press, 1992).
- ¹³J. Frenkel, *Phys. Rev.* **54**, 647 (1938).
- ¹⁴S. D. Ganichev, E. Ziemann, W. Prettl, I. N. Yassievich, A. A. Istratov, and E. R. Weber, *Phys. Rev. B* **61**, 10361–10365 (2000).
- ¹⁵O. V. Feklisova, E. B. Yakimov, and N. A. Yarykin, *Semiconductors* **36**, 282–285 (2002).
- ¹⁶N. Baber, H. Scheffler, A. Ostmann, T. Wolf, and D. Bimberg, *Phys. Rev. B* **45**, 4043–4047 (1992).
- ¹⁷Q. S. Zhu, K. Hiramatsu, N. Sawaki, I. Akasaki, and X. N. Liu, *J. Appl. Phys.* **73**, 771–774 (1993).
- ¹⁸Y. Kamiura, K. Fukuda, S. Ohyama, and Y. Yamashita, *Jpn. J. Appl. Phys., Part 1* **39**, 1098–1099 (2000).